JOURNAL OF MATERIALS SCIENCE 30 (1995) 5251–5258

Structure and properties of aligned short fibre-reinforced intermetallic matrix composites

D. E. ALMAN*, N. S. STOLOFF
Materials Engineering Department, Rensselaer Polytechnic Institute, Troy, NY 12180, USA
A. BOSE
Research and Development, Parmatech Corporation, Petaluma, CA 94954, USA
R. M. GERMAN
Department of Engineering Science and Mechanics, The Pennsylvania State University, University Park, PA 16802, USA

Powder injection moulding techniques were utilized to align short fibres (Al_2O_3 and SiC) in a variety of intermetallic matrices (NiAl, $MoSi_2$ and $TaTiAl_2$). The alignment was accomplished by extruding a mixture of powders and short fibres with a polymer-based binder through a constricting nozzle. The binder was removed and the powder and fibres were consolidated, producing an aligned short fibrous composite. The effects of powder morphology, fibre volume fraction and fibre diameter on the alignment were demonstrated. Small diameter powders were required to ensure alignment of an appreciable loading of fibres in a powder matrix. Tensile and hardness tests were used to evaluate the effectiveness of the aligned short fibres to strengthen and toughen the matrices. The mechanical behaviour of these aligned short fibrous composites were found to be comparable to similar aligned continuous fibrous composites produced by conventional techniques.

1. Introduction

Many intermetallic compounds offer an attractive combination of low density, high melting point and resistance to oxidation, which are extremely desirable for high-temperature structural materials. However, the lack of adequate low-temperature toughness and poor creep resistance of these compounds have limited their use for engineering applications. These deficiencies have been addressed through alloying and composite strengthening. Microalloying has been successful in improving the low-temperature ductility, hence toughness, of only a few specific compounds (i.e. $Ni_3Al + B$ and $Ni_3Si + B$). Macroalloying also has been successful sometimes, as in the $(Fe,Ni)_3V$ series alloys. Composite strengthening, on the other hand, can be applied to improve the toughness and creep resistance of practically any compound. Thus, over the last decade or so there has been interest in using intermetallic alloys as matrix materials for high-temperature structural composites.

In general, intermetallic compounds exhibit a brittle-to-ductile transition with increasing temperature. Below the transition temperature the compounds are brittle and above the transition temperature they exhibit poor creep resistance. Composite strengthening can improve these deficiencies, particularly with aligned fibres. It is well known that a brittle fibre can strengthen a ductile matrix (an intermetallic compound above the transition temperature) if a strong interface exists between the fibre and matrix [1]. It is also well known that a brittle fibre can toughen a brittle matrix (an intermetallic compound below the transition temperature) through various mechanisms such as fibre debonding, pull-out and crack deflection [1].

Solid state powder metallurgical (P/M) processing is an ideal route for fabricating high-temperature structural composites. P/M techniques have been developed for fabricating aligned continuous reinforced intermetallic–matrix composites [2–5]. Powder injection moulding (PIM) techniques can be used to align short fibres in a powder matrix [6–11]. An advantage of this technique is that with proper die design, complicated near-net-shaped aligned fibrous composites can be produced [8, 9].

The PIM technique as applied to processing aligned fibre-reinforced composites is basically a four-step process; feedstock preparation, extrusion for fibre alignment, debinding, and consolidation. Feedstock preparation consists of mixing the powder and chopped fibres with a polymer binder. The feedstock is heated above the softening point of the binder and either extruded through a tapered die or injected into a mould cavity. As long as the flow of the feedstock converges, the fibres will orient parallel to the direction of the feedstock flow. The binder is then removed

* *Present address*: U.S. Bureau of Mines, Albany, OR 97321, USA.

0022–2461

TABLE I Properties of intermetallic matrices

Matrix	Density ($g\,cm^{-3}$)	Melting point (°C)	Brittle to ductile transition temperature (°C)
NiAl	5.86	1640	400–600
$MoSi_2$	6.25	2030	900–1300
$TaTiAl_2$	7	> 1800	?

and the composite is consolidated to produce an aligned short fibre-reinforced composite.

This paper discusses research on a variety of intermetallic matrices (NiAl, $MoSi_2$ and $TaTiAl_2$, see Table I for typical properties of these matrices) reinforced with aligned short ceramic fibres (Al_2O_3 and SiC). The effects of powder morphology, fibre volume fraction and fibre diameter on the alignment of fibres in a powder matrix were addressed. The mechanical behaviour (tensile and hardness) of these composites were evaluated and compared to the properties available in the literature of similar composites consolidated by conventional techniques.

2. Experimental procedure

2.1. Materials

The characteristics of the fibres and powders used are summarized in Table II. The matrix of NiAl composites was synthesized from a stoichiometric mixture of nickel and aluminium powders using reaction synthesis techniques, which are described in detail elsewhere [8]. $MoSi_2$ and $TaTiAl_2$ matrix composites were fabricated from prealloyed powders by conventional pressure-aided sintering techniques. The morphologies of the powders used are shown in Fig. 1. Notice all the powders were small; however, the morphologies of the nickel and aluminium powders were spherical and the prealloyed $MoSi_2$ and $TaTiAl_2$ powders were irregular. Two fibres were used for this study, the DuPont FP Al_2O_3 fibre (Fig. 2) and the Textron SCS-6 SiC fibre. The fibres were chopped from a continuous spool, and had an aspect ratio ranging from 10–100.

2.2. Feedstock preparation

An appropriate amount of fibres was blended with the powders to produce composites with fibre loadings of either 10, 15 or 20 vol %. To aid the dispersion of the fibres in the powder matrix, an alcohol slurry was produced for blending. The slurry was mixed for 1 h with a Turbula type mixer, after which the alcohol was allowed to evaporate. The feedstock was prepared by incorporating the fibre/powder blend into a polymer binder (based on low molecular weight polypropylene, paraffin, carnauba wax, and stearic acid). The fibre/powder blend was added to the melted binder while being mixed in a small double planetary-type mixer. The feedstock contained approximately 30 vol % binder.

TABLE II Characteristics of powders and fibres

		Source/designation	Shape	Average particle size[a] (μm)
Powder	Ni	Novamet/4SP	Spherical	3
	Al	Valimet/H-3	Spherical	3
	$MoSi_2$	H.C. Stark/grade C	Irregular	4
	$TaTiAl_2$	Pratt and Whitney/atomized	Irregular	9
Fibre				
	Al_2O_3	DuPont/FP		20[b]
	SiC	Avco-Textron/SCS-6		127[b]

[a] Determined by laser light scattering technique.
[b] Fibre diameter.

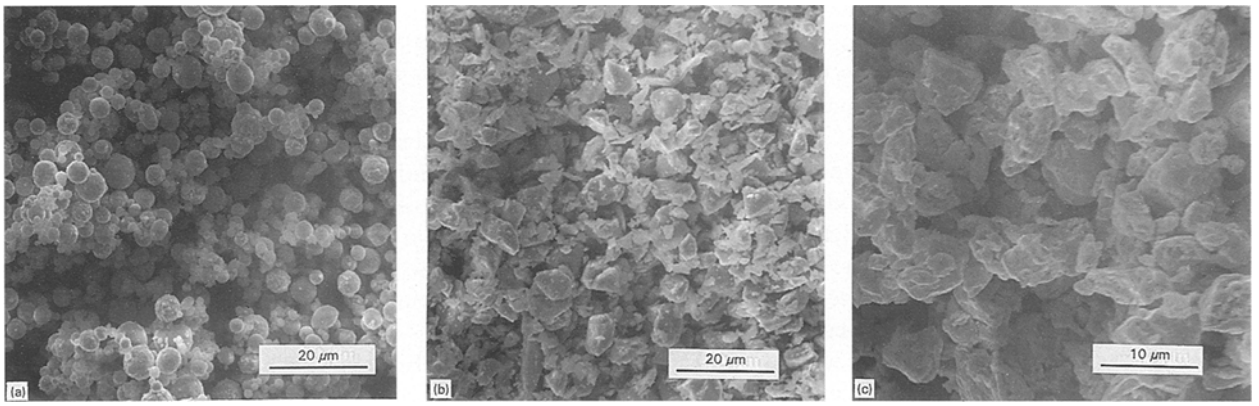

Figure 1 Morphologies of the powders used: (a) spherical elemental nickel and aluminium powders; (b) irregular $MoSi_2$ powders; and (c) irregular $TaTiAl_2$ powders.

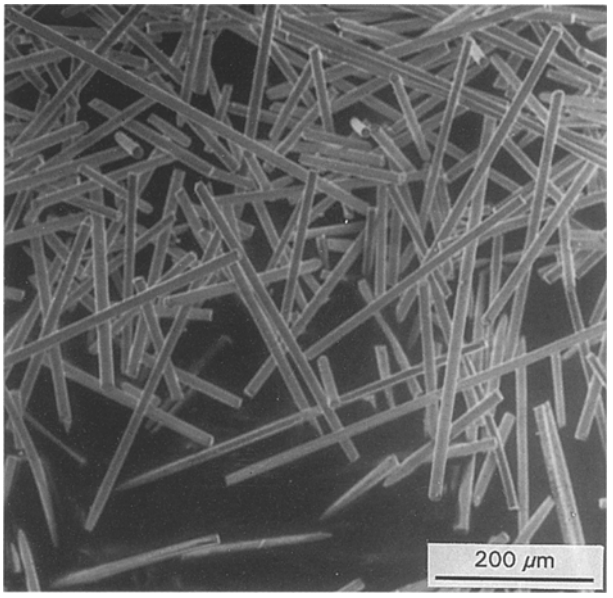

Figure 2 Chopped DuPont-FP Al_2O_3 fibres.

2.3. Fibre alignment

Fibre alignment was achieved by extruding the feedstock, heated to above the softening point of the binder (90 °C), through a constricted nozzle. For $TaTiAl_2$ and $MoSi_2$ matrix composites, a small extrusion nozzle was employed that was tapered from 12.7 mm to 1.5 mm. This produced "wires" of powder and fibre of roughly 1.5 mm diameter. A number of these "wires" were placed in a cylindrical mould bag and cold isostatically pressed (CIP) at 210 MPa to produce a specimen roughly 12.7 mm diameter by 25 mm long. Complete details on this extrusion plus CIP technique can be found in previous publications [8–10]. For NiAl matrix composites, a larger extrusion nozzle was employed, which reduced in diameter from 51 mm to 12.7 mm. This eliminated the need for CIPing and avoided any misalignment due to errors in placement of the "wires" in the mould bag. However, a larger quantity of feedstock was required (200 g for the large nozzle as opposed to 50 g for the small nozzle).

2.4. Debinding and consolidation

All samples were placed in fine Al_2O_3 wicking powder prior to debinding. The binder was thermally removed in flowing hydrogen by heating the specimens at a rate of 2 °C min^{-1} to 450 °C. After 300 min at 450 °C the specimens were allowed to furnace cool. After debinding, NiAl matrix composites were placed in a vacuum furnace and reactively sintered at 750 °C for 15 min. $MoSi_2$ and $TaTiAl_2$ matrix composites were conventionally sintered in vacuum at 1200 °C for 1 h.

Final consolidation occurred by hot isostatic pressing (HIPing). NiAl and $TaTiAl_2$ matrix composites were vacuum encapsulated in a 304 stainless steel can and HIPed at 1250 °C and 172 MPa for 2 h. $MoSi_2$ matrix composites were vacuum encapsulated in titanium HIP cans (inner walls lined with niobium foil) and HIPed at 1500 °C and 172 MPa for 2 h. In an attempt to minimize any cracking due to mismatches between thermal expansion coefficients (CTE mismatch) of the matrices and fibres, cooling and depressurization occurred slowly (from processing temperature to 300 °C over 60 min, with the pressure decreasing only as a result of the decreasing temperature; over the next 60 min cooling and depressurization to atmospheric conditions).

2.5. Microstructural evaluation and mechanical testing

The microstructures of the composites were evaluated by standard metallographic techniques employing optical and scanning electron microscopy. The mechanical behaviour of the composites was evaluated by hardness and tensile testing. The properties of similarly consolidated monolithic matrix materials also were evaluated. Only monolithic NiAl and a NiAl/15 vol % Al_2O_3 FP short fibrous composite were tested in tension. Cylindrical dog-bone type tensile specimens were electro-discharged machined from the HIPed ingots. The gauge section of each specimen was 3.18 mm diameter by 19.1 mm length, with an overall reduced section of 25.4 mm length. The grip sections were 6.98 mm diameter and the entire length of the tensile specimen was approximately 38.2 mm. Prior to testing, the surface of the specimens was mechanically polished using a 0.3 μm Al_2O_3 paste and ultrasonically cleaned in a mixture of alcohol and acetone. Testing was performed at 700 and 800° C in air with a servo-hydraulic Instron machine at a constant crosshead displacement of 0.2 mm min^{-1}, which corresponds to an initial strain rate of 1.67×10^{-4} s^{-1}. Rockwell "A" hardness tests were used to evaluate the $MoSi_2$ and $TaTiAl_2$ composites.

3. Results and discussion

3.1. Microstructural features

Typical microstructures of the PIM composites are shown in Figs 3–5 for NiAl, $MoSi_2$ and $TaTiAl_2$ matrix composites, respectively. Notice, that the fibre alignment appears suitable in all the composites regardless of the starting powder morphology, spherical for NiAl and irregular for $MoSi_2$ and $TaTiAl_2$. These results indicate that powder morphology is not critical for alignment of fibres in a powder matrix. In a previous publication, German and Bose [6], reported that the alignment of fibres in a powder matrix was superior when small spherical powders (5 μm) were used as opposed to large spherical powders (70 μm). Thus, it appears that powder size plays a larger role in alignment process than does powder morphology. However, powder morphology can effect the rheological behaviour of the feedstock during extrusion or injection moulding [10]. Because many intermetallic powders are not available in small sizes, the elemental powder approach of reactive synthesis for consolidation appears ideally suited for coupling with binder-assisted extrusion or injection moulding. Elemental powders tend to be readily available in small sizes.

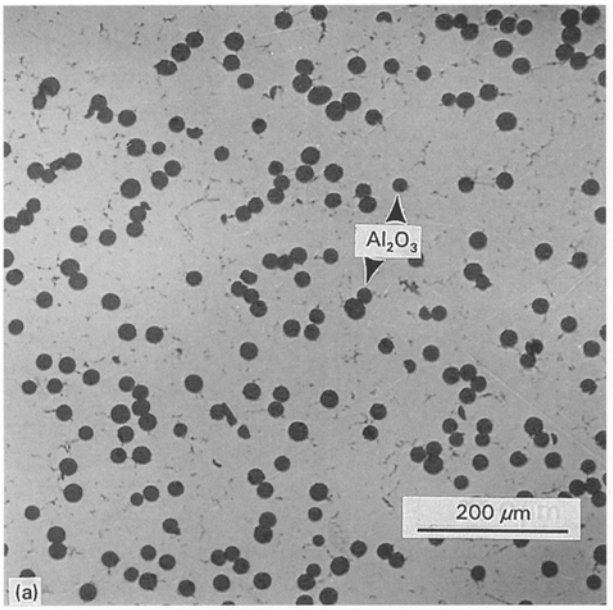

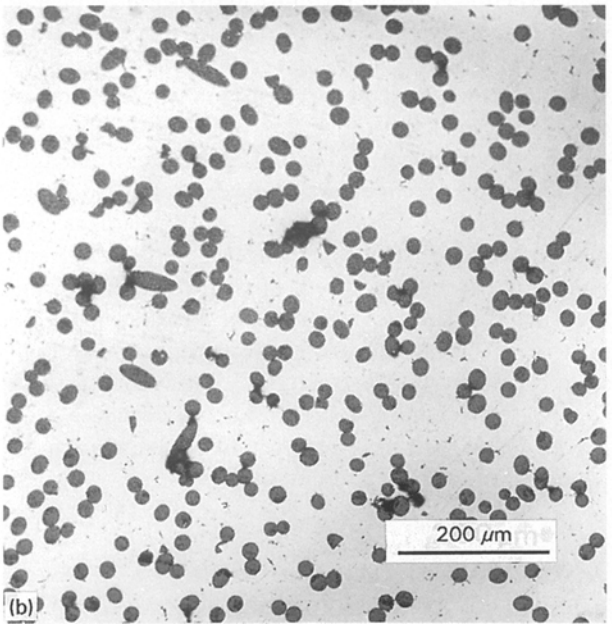

Figure 3 Microstructure of $NiAl/Al_2O_3$ aligned short fibrous composites: (a) NiAl/10 vol % Al_2O_3 fibres; (b) NiAl/20 vol % Al_2O_3 fibres. Note the misaligned fibres in the 20 vol % composite.

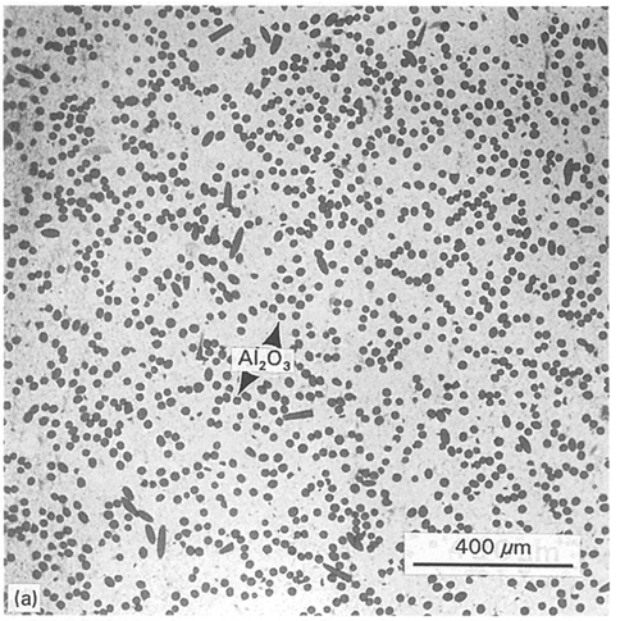

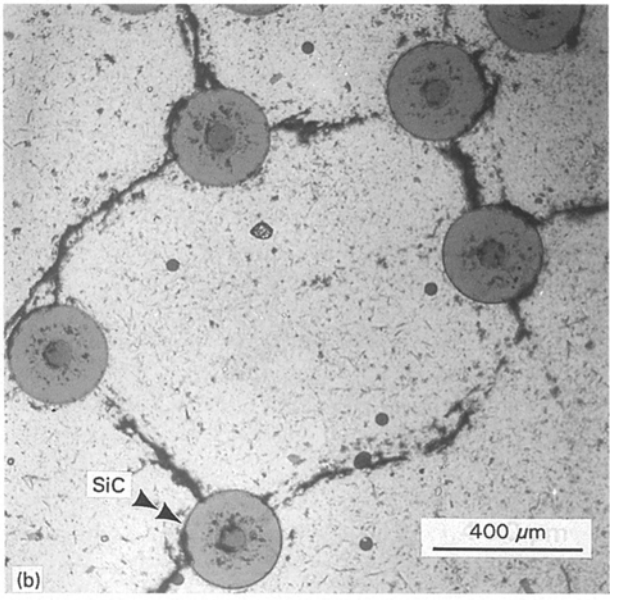

Figure 4 Microstructure of $MoSi_2$ composites: (a) $MoSi_2$/20 vol % Al_2O_3 fibres (20 μm diameter); (b) $MoSi_2$/5 vol % SiC fibres (127 μm diameter). Note that both the large and small diameter fibres were aligned.

Both the large diameter (SCS-6 fibres) and the small diameter (FP fibres) have been aligned by this process (Fig. 4). The cracking around the SCS-6 fibre in the $MoSi_2$ matrix is due to the CTE mismatch between the SiC fibre and the matrix, and has been observed in other studies on this system [3]. The effect of fibre volume fraction is assessed in the microstructures shown in Fig. 3. Notice that the agglomeration and the misalignment appears to increase in the higher volume fraction composite.

A simple geometric based model shows the interdependency of powder size, fibre size, fibre volume fraction and the alignment of fibres in any powder matrix. As shown in Fig. 6, for fibre alignment to occur, the maximum size of the powder can be no greater than the edge-to-edge distance between the fibres, λ. Assuming a uniform fibre distribution, λ is

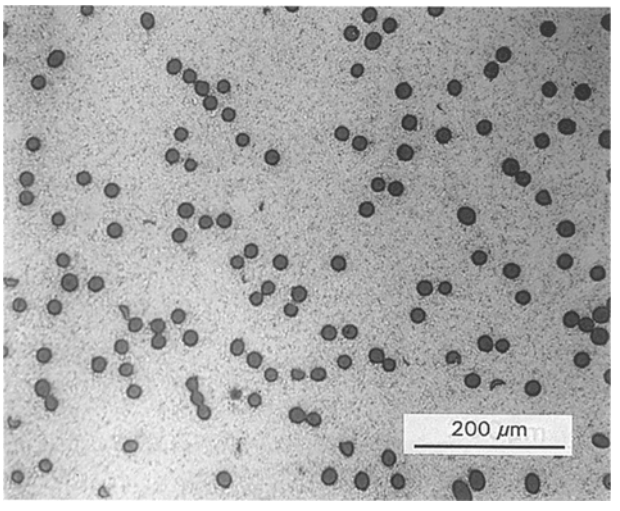

Figure 5 Microstructure of $TaTiAl_2$/10 vol % Al_2O_3 composite.

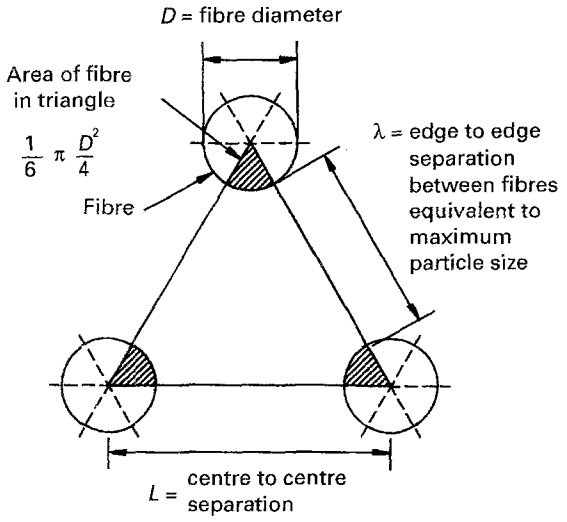

1. Area of the three fibres in the defined geometric element (triangle), which is representative of the composite microstructure

$$A_f = \frac{1}{6}\pi\frac{D^2}{4}3$$

2. Area of triangle

$$A_T = \frac{1\sqrt{3}}{2\ 2}L^2$$

3. Volume fraction of fibres in triangle

$$v_f = \frac{A_f}{A_T} = \frac{\pi D^2}{2\sqrt{3}\,L^2}$$

4. If volume fraction is known, then

$$L = (\pi D^2 / 2\sqrt{3}\,v_f)^{1/2}$$

5. λ = maximum particle size

$$\lambda = L - D$$

$$\lambda = (\pi D^2 / 2\sqrt{3}\,v_f)^{1/2} - D$$

Figure 6 Derivation of the relationship between powder size, fibre diameter and volume fraction on the alignment of fibres in a powder matrix.

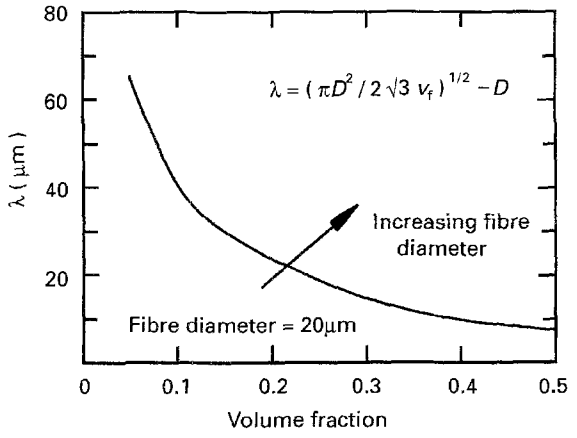

Figure 7 Effect of fibre volume fraction on the powder size required for alignment.

the difference between the centre-to-centre fibre separation, L, and two fibre radii (or the fibre diameter, D)

$$\lambda = L - D \tag{1}$$

The fibre volume fraction v_f, can be expressed as the area fraction of fibres in a defined geometric element that is representative of the microstructure (the triangle in Fig. 6); thus

$$v_f = \frac{\pi D^2}{2\sqrt{3L^2}} \tag{2}$$

Rearranging and substituting into Equation 1 gives

$$\lambda = \left(\frac{\pi D^2}{2\sqrt{3}v_f}\right)^{1/2} - D \tag{3}$$

which relates maximum allowable powder particle size for fibre alignment to fibre diameter and volume fraction. This model should be treated as a first approximation, as it does not account for factors, such as fibre length and particle packing density, which can effect alignment. Other parameters such as die design and binder loading, also are not considered. Further, the model is based upon a uniform fibre distribution, which is not typical of the PIM composite microstructure (Figs 3–5) or, for that matter, composites produced through powder infiltration techniques (see, for instance, Figs 1 and 8 in [5] and Fig. 2 in [4]). However, it demonstrates that for significant volume fractions of fibres to be aligned in a powder matrix (either through PIM or powder infiltration), small-diameter particles are required, especially for small-diameter fibres like the 20 μm diameter DuPont FP Al_2O_3 fibre (Fig. 7).

3.2. Mechanical properties

The tensile behaviour of NiAl/15 vol % Al_2O_3 fibres and monolithic NiAl are summarized in Table III. The strain-to-failure was calculated from the gauge length and crosshead displacement; note that these values correlate well with the reduction in area measured from the specimens. The fracture energies were estimated from the area under the load–displacement curves.

At 700 °C, monolithic NiAl failed in a brittle manner (Fig. 8). At this temperature, the addition of the FP fibres did not toughen NiAl, as indicated by the strain-to-failure, reduction in area and the estimated fracture energy (Table III). Fracture surfaces revealed that the short Al_2O_3 fibres remained well bonded to the NiAl matrix with little or no occurence of fibre/matrix debonding and fibre pullout (Fig. 9). At 800 °C, monolithic NiAl displayed considerable ductility and in fact failed in a ductile manner (Fig. 10). The fibres only marginally strengthened the matrix at this

TABLE III Tensile properties[a] of NiAl and NiAl/15 vol% aligned short Al_2O_3 (Dupont FP) fibrous composite

	Temp. (°C)	σ_{ys} (MPa)	σ_{UTS} (MPa)	ε_f[b] (%)	R.A.[c] (%)	Fracture[d] energy (J cm^2)
NiAl	700	173	191	4	3	4.8
NiAl + Al_2O_3 fibres	700	196	196	< 1	0	1.4
NiAl	800	135	154	14	13	39
NiAl + Al_2O_3 fibres	800	142	163	5.6	3	18

[a] Results of tensile tests were recorded at load versus crosshead displacement.
[b] ε_f = strain to failure measured from load–displacement curve and specimen gauge length.
[c] R.A. = reduction in area measured directly from specimen.
[d] Fracture energy estimated from area under load–displacement curves.

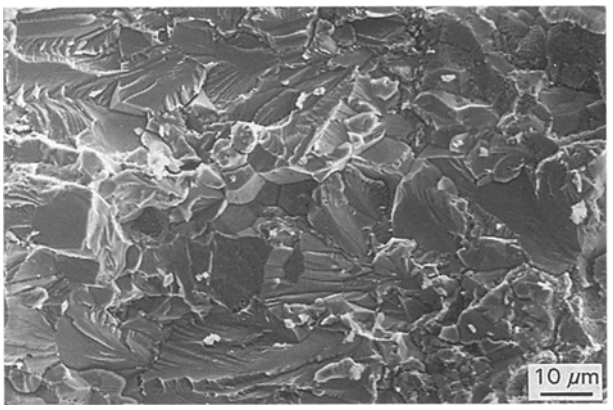

Figure 8 Fracture surface of monolithic NiAl tested in tension at 700 °C.

temperature. Fracture surfaces showed that the fibres separated from the matrix (Fig. 11), and thus limited the strain-to-failure of the composite.

It is interesting to compare the behaviour of the short fibrous composite with the behaviour of a NiAl matrix–Al_2O_3 (DuPont FP) continuously aligned fibrous composite produced through powder infiltration [5, 12]. The fracture surfaces of the continuous aligned fibrous composites were remarkedly similar to the PIM short fibrous composites (comparing Figs 9 and 11 with Fig. 4 in [5] or Fig. 6 in [12]). The addition of continuously aligned DuPont FP Al_2O_3 fibres did not toughen NiAl in bending below the DBTT (13 MPa m$^{1/2}$ compared to 14 MPa m$^{1/2}$ for the monolithic NiAl and NiAl/Al_2O_3 continuous aligned fibrous composite at room temperature, respectively) [5, 12]. The bend fracture surfaces displayed little or no debonding and pullout of the continuous fibres [5, 12], similar to the tensile fracture surfaces of the short fibrous composite. At 1200° C the addition of the continuous aligned fibres did, in fact, significantly strengthen NiAl in bending [5, 12]. However, the fracture surfaces at this temperature also resembled that of the aligned short fibrous composite tested in tension at 800 °C, with the fibres separating from the matrix.

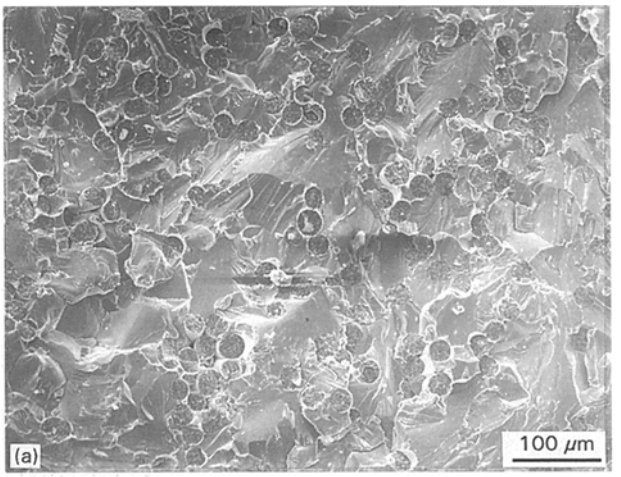

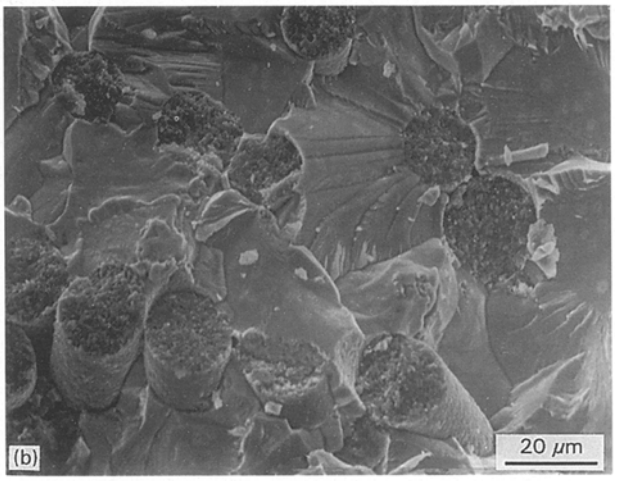

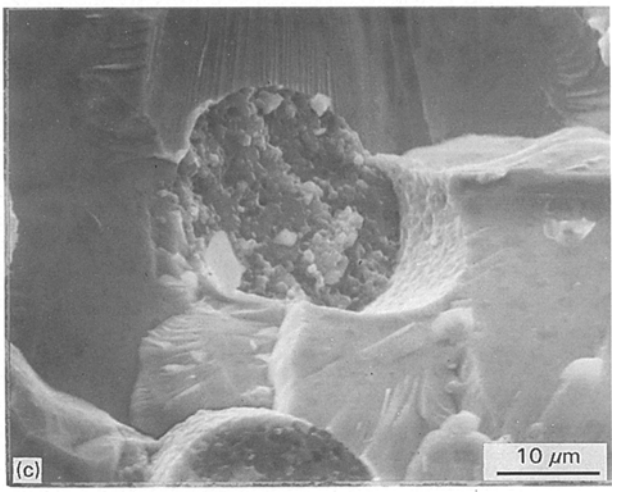

Figure 9 Views of the fracture surfaces of a NiAl/15 vol % aligned fibrous composites tested in tension at 700 °C at various magnifications. Note the fibres remain bonded to the matrix with limited fibre pullout occurring.

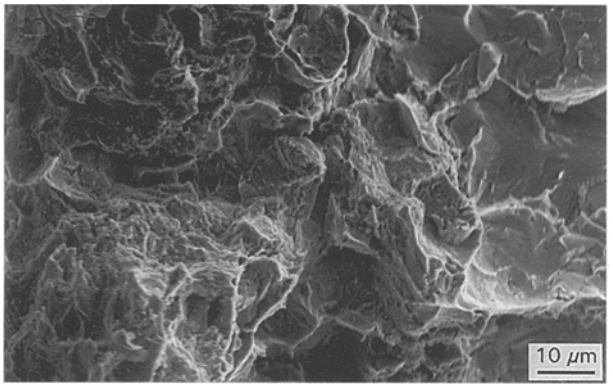

Figure 10 Fracture surface of monolithic NiAl tested in tension at 800 °C.

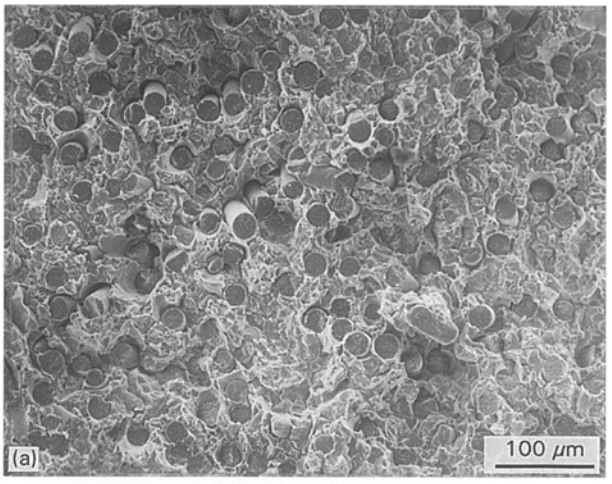

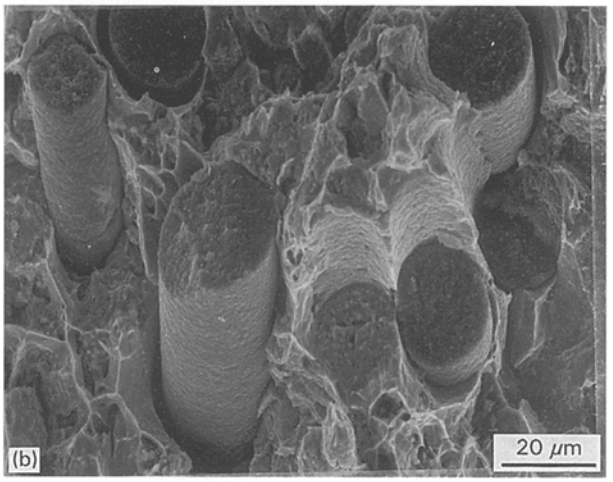

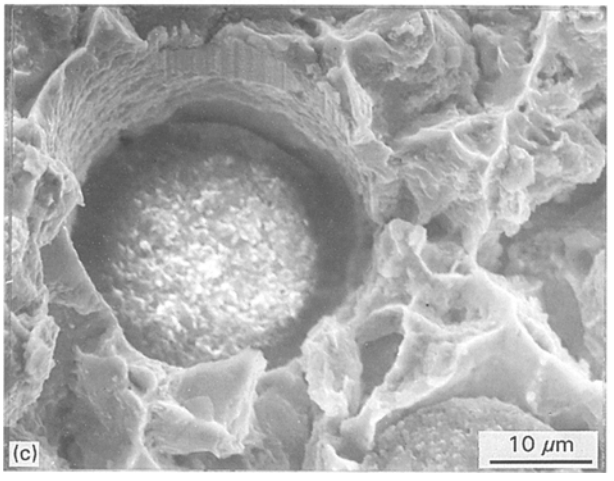

The behaviour of a fibrous composite is governed by the aspect ratio of the fibre and the fibre–matrix interfacial strength. Because the fracture behaviour (i.e. fibre/matrix debonding and fibre pullout) of the short fibrous and continuous fibrous composites were similar, the failure of the PIM $NiAl/Al_2O_3$ FP fibre composites to be "tougher" than monolithic NiAl should not be attributed to the aspect ratio of the fibres but instead to the interfacial strength. In fact, the strength of the $NiAl/Al_2O_3$ interface is quite strong ($\tau_i = 280$ MPa at room temperature [13]). Composite theory suggests that the maximum work due to pullout will occur when the fibre length, l, is equal to its critical length, l_c, for pullout ([1] pp. 232–8). When $l < l_c$, the work of fracture increases with fibre length because of the increase in fibre length being pulled out [1]. When $l > l_c$, the work of fracture decreases as fibre breaks intervene and fibre pullout decreases [1]. The critical fibre length, l_c, can be calculated from the ultimate fibre strength, σ_{fu}, and the interfacial strength, as [1]

$$l_c = \left(\frac{\sigma_{fu}}{4\tau_i}\right) d \tag{4}$$

where d is the fibre diameter. For the 20 μm diameter DuPont FP Al_2O_3 fibres embedded in an NiAl matrix, the critical length is calculated as 25 μm ($\sigma_{fu} = 1380$ Mpa for the FP fibre [14]). The length of the fibres used to prepare the PIM composites was greater than this value. Clearly, the interface that develops between NiAl and the FP-Al_2O_3 fibres is too strong for toughening to be derived from the FP fibres. For strengthening an intermetallic matrix at temperatures above the DBTT with a brittle fibre, a strong fibre/matrix interface is desired. The long fibres appear more suited for strengthening at elevated temperatures than the short fibres. However, this may be more of a function of fibre loading, as the short fibrous composites only contained 15 vol % fibres (present study), whereas the continuous fibrous composites typically contained upwards of 35 vol % [4].

Owing to limited quantities of material, tensile specimens could not be machined from the PIM $TaTiAl_2/Al_2O_3$ and $MoSi_2/Al_2O_3$ composites. Hardness tests were used to evaluate these composites. Fig. 12 shows hardness indentations in monolithic $TaTiAl_2$, a $TaTiAl_2$/10 vol % Al_2O_3 particulate composite and a $TaTiAl_2$/10 vol % Al_2O_3 PIM aligned fibrous composite. Notice that large craters of fractured material adjacent to the indents are absent from the fibrous composite. These craters are present in both the monolithic and particle composite materials. Monolithic $MoSi_2$ and $MoSi_2/Al_2O_3$ PIM composite behaved in a similar manner to the monolithic $TaTiAl_2$ and $TaTiAl_2/Al_2O_3$ PIM composite, respectively. This would suggest that the short fibres may

Figure 11 Views of the fracture surfaces of a NiAl/15 vol % aligned fibrous composites tested in tension at 800° C at various magnifications. Note the fibres separated from the NiAl matrix.

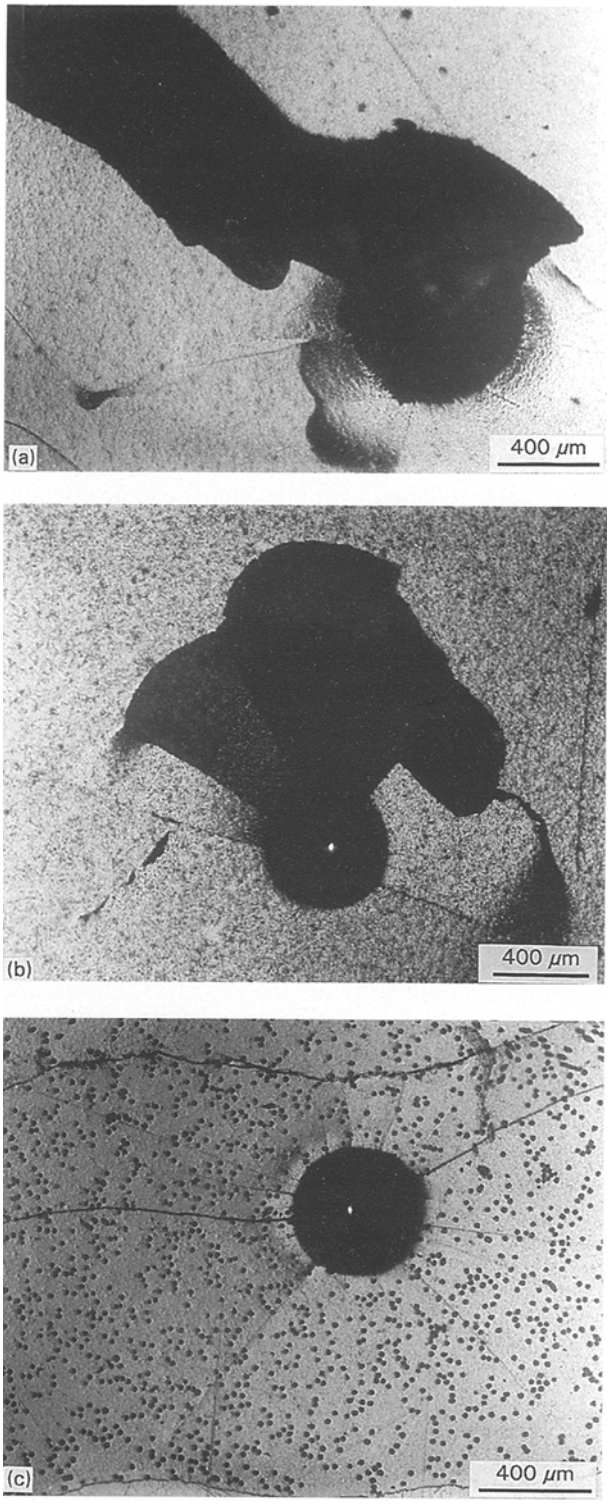

Figure 12 Hardness indentations in (a) monolithic $TaTiAl_2$; (b) $TaTiAl_2$/10 vol % Al_2O_3 particulate composite; and (c) $TaTiAl_2$/10 vol % Al_2O_3 aligned short fibrous composite. Note the absence of craters adjacent to the indent in the fibrous composite, which are present in the monolithic material and particulate composite.

toughen these matrices. Clearly, further research is required.

4. Conclusion

The alignment of short fibres in a variety of intermetallic matrices by PIM techniques was successfully accomplished. Composites with upwards of 20 vol % fibres were produced. Both large and small diameter fibres were aligned in a powder matrix. Small irregular and spherical powders were used. In general, small diameter powders are required to facilitate fibre alignment. The addition of the short FP fibres did not improve the toughness of an NiAl matrix. However, this was attributed to the strong interface that develops between the matrix and fibre and not the fibre length. In fact, tensile fracture surfaces (present study) resembled the fracture surfaces (in bending) of long FP fibre–NiAl matrix composites [5, 12]. Thus, the PIM technique is viable for producing aligned fibrous composites.

Acknowledgements

This research was supported by the Defense Advanced Research Projects Agency (DARPA) and the Office of Naval Research (ONR) through Contract N00014-86-K-0770. The authors thank Dr M.J. Maloney, Pratt and Whitney, FL, for supplying the $TaTiAl_2$ powders, and Dr M.F. Henry, GE Corporate Research and Development, for supplying the SCS-6 fibres.

References

1. K. K. CHAWLA "Composite Materials" (Springer, Berlin, 1987).
2. P. K. BRINDLEY, in "High Temperature Ordered Intermetallic Alloys II", edited by N. S. Stoloff, C. C. Koch, C. T. Liu and O. Izumi, MRS Symposium Proceedings Vol. 81 (MRS, Pittsburgh, PA, 1987) p. 419.
3. M. J. MALONEY and R. J. HECHT, *Mater. Sci. Eng.* **A155** (1992) 19.
4. D. L. ANTON, in "High Temperature/High Performance Composites", edited by F. D. Lemkey, S. G. Fishman, A. G. Evans and J. R. Strife, MRS Symposium Proceedings Vol. 120 (MRS, Pittsburgh, PA, 1988) p. 57.
5. D. M. SHAH and D. L. ANTON, in "Proceedings of the First International Symposium on Structural Intermetallics", edited by R. Darolia, J. J. Lewandowski, C. T. Liu, P. L. Martin, D. B. Miracle and M. V. Nathal (TMS, Warrendale, PA, 1993) p. 755.
6. R. M. GERMAN and A. BOSE, *Mater. Sci. Eng.* **A107** (1989) 107.
7. A. BOSE and R. M. GERMAN, *Adv. Mater. Manuf. Process* **3** (1988) 37.
8. D.E. ALMAN and N.S. STOLOFF, *Int. J. Powder Metall.* **27** (1) (1991) 29.
9. D. E. ALMAN and N. S. STOLOFF, in "Low Density, High Temperature Powder Metallurgy Alloys", edited by W. E. Fraizer *et al.* (TMS, Warrendale, PA, 1991) p. 109.
10. A. BOSE, D. E. ALMAN and N. S. STOLOFF, in "Advances in Powder Metallurgy and Particulate Materials – 1992", Vol. 9, "Particulate Materials and Processes", edited by J. M. Capus and R. M. German (MPIF/APMI, Princeton, NJ, 1992) p. 209.
11. R. M. GERMAN, "Powder Injection Moulding" (MPIF/APMI, Princeton, NJ, 1990).
12. D. L. ANTON and D. M. SHAH, in "Intermetallic Matrix Composites II", edited by D. B. Miracle, D. L. Anton and J. A. Graves, MRS Symposium Proceedings Vol. 273 (MRS, Pittsburgh, PA, 1992) p. 157.
13. R. R. BOWMAN, *ibid.*, p. 145.
14. J. C. ROMINE, *Ceram. Engr. Sci. Proc.* **8** (7–8) (1987) 755.

Received 1 June 1994
and accepted 11 April 1995